



Contents lists available at ScienceDirect

# Construction and Building Materials

journal homepage: [www.elsevier.com/locate/conbuildmat](http://www.elsevier.com/locate/conbuildmat)

## Self-healing characterization of UHPFRCC with crystalline admixture: Experimental assessment via multi-test/multi-parameter approach



Francesco Lo Monte\*, Liberato Ferrara

Department of Civil and Environmental Engineering, Politecnico di Milano, Milan, Italy

### HIGHLIGHTS

- The adoption of strain-hardening cement composites significantly promotes self-healing.
- Multi-test approach for self-healing assessment appeared to be robust in durability monitoring.
- Self-healing is very effective already after 1 month of curing for the UHDC studied.
- The mixes showed sizable self-healing with even almost full crack-sealing after 6 months.
- Re-cracking has a detrimental effect in self-healing for all the considered parameters.

### ARTICLE INFO

#### Article history:

Received 2 November 2020

Received in revised form 13 January 2021

Accepted 29 January 2021

#### Keywords:

Aggressive environment

Bending

Crack sealing

Durability

Permeability

Self-healing

Tension

Ultra high durability concrete – UHDC

### ABSTRACT

Within the framework of the Research Project ReSHEALience, new advanced Ultra High-Performance Fibre-Reinforced Cement Composites with enhanced durability, hereafter denoted as Ultra High Durability Concretes, are under investigation to characterize their tensile behaviour and durability performance in aggressive conditions, devoting particular attention to the phenomenon of self-healing. Three different mixes are under scrutiny, based on the combination of cement (CEM I or CEM III), slag, small aggregates (sand with a maximum size of 2 mm), and steel or metallic-alloy amorphous fibre. Self-healing capability has been investigated in aggressive environment (namely, under immersion in geothermal water) via 3 different test setups: (1) water permeability test on pre-cracked concrete disks, (2) 4-Point Bending Test – 4PBT on  $100 \times 100 \times 500\text{mm}^3$  prismatic beam specimens and (3) on  $25 \times 100 \times 500\text{mm}^3$  thin beams. In the case of beams, self-healing has been assessed via visual inspection of cracks through digital microscope and via mechanical re-loading, so to investigate both crack-sealing capability and mechanical recovery. The results of this assessment aim at providing the starting point for a data base finalized at defining a design approach explicitly taking into account self-healing in the evaluation of structural durability. In particular, it has been observed as the adoption of strain-hardening cement composites significantly promotes self-healing phenomenon, thanks to smeared cracking in the tensile region and to consequent low values of crack opening. Self-healing proved to be very effective already after 1 month of curing.

© 2021 The Authors. Published by Elsevier Ltd. This is an open access article under the CC BY-NC-ND license (<http://creativecommons.org/licenses/by-nc-nd/4.0/>).

### 1. Introduction

Many structures and infrastructures in the world are exposed to Extremely Aggressive Environments (EAE) characterized by chemical (such as presence of sulphate or chlorides), physical (as for example freeze and thaw cycles) and mechanical (such as abrasion) attacks. This makes of major importance the durability performance, broadly meant as the capacity of the structure to

retain its level of performance throughout the intended service life. Within this context, durability has an important economic impact if early and continuous repairs are needed, so dramatically increasing the initial building cost [1].

When exposed to EAE, the proper choice of materials in the design phase accordingly to the specific structural application can lead to structures much more durable, with improved performance in time and far less need of repair interventions. Such approach implies a final reduction of costs even though a larger initial investment can be required.

In this context, it becomes intriguing the application of advanced materials, such as Ultra High Performance Fibre

\* Corresponding author at: Department of Civil and Environmental Engineering, Politecnico di Milano, Piazza Leonardo da Vinci 32, 20133 Milan, Italy.

E-mail address: [francesco.lo@polimi.it](mailto:francesco.lo@polimi.it) (F. Lo Monte).

Reinforced Cementitious Composites (UHPRCC), in which engineered additions can help in improving peculiar aspects linked to special applications, according to the principle of tailorability. These advanced materials, however, are still not properly addressed in standards and codes, with the consequent limitation of their use in practice [2]. Moreover, their durability has been so far mostly addressed with reference to the un-cracked state whereas its proper assessment in the cracked structural service state is so far lacking [3].

In order to push in such promising direction, the Research Project ReSHEALience has been launched in 2018 within the framework of the European Science and Innovation Programme Horizon 2020 (GA 760824), involving 14 Partners all around Europe.

The objective of the Project is to present a new approach for structural design, based on durability (Durability-Assessment based Design – DAD) and Life Cycle Assessment (LCA). New advanced UHPRCC with improved durability (thus called also Ultra-High Durable Concretes – UHDCs in the following) are under investigation to characterize the tensile behaviour and the durability performance in aggressive conditions. In this context, self-healing, namely the capability of concrete to self-seal cracks and to recover its mechanical and durability properties, plays a major role [4,5].

The three mixes studied are based on the combination of cement type CEM I or type CEM III, with slag, fine aggregates (sand with a maximum size of 2 mm) and steel or metallic-alloy amorphous fibres (employed at dosages around 1.5% by volume). In all the mixes, crystalline admixture has been added since it acts as porosity reducer and self-healing promoter [6–8].

One of the main features of such UHDCs is strain-hardening behaviour in direct tension, with the consequent uniform stable multiple cracking in un-notched elements. Such property allows to keep the opening of each single crack very narrow even for high values of residual tensile strain, this being instrumental for significantly improving the durability of concrete structures in the cracked state.

The material concept relies upon a micro-mechanical design of the mix composition, based on the balance between crack-tip toughness and fibre pull-out work [9–11]. Once the first crack is formed, the crack bridging action of the fibres is activated. As above mentioned, this results into a signature tensile behaviour characterized by stable multiple cracking process and strain-hardening response, up to the onset of the unstable localization of one single crack [12]. Moreover, the synergy between crack tightness and material composition also results into a high propensity to autogenous self-healing, with synergetic effects on the enhancement of material and structural durability [13–29].

Healing products reconstruct (partially or totally) the through-crack continuity also improving the fibre–matrix bond, this even leading to the formation of new cracks instead of the re-opening of the healed one in case of reloading [19]. This concept is of the utmost importance in assessing the material and structural durability of the aforesaid broad category of cementitious composites when employed in real applications in the cracked serviceability state.

As remarked above, the “superior” durability of UHPRCCs has been so far mostly addressed in the un-cracked state, as an “obvious” outcome of the very low porosity of the material, featuring a highly compacted matrix because of its peculiar composition. Few studies have started being published in the very last years [30,31] addressing the issue of durability in the cracked state and highlighting the consequent importance of self-healing. In this respect, the mechanisms of self-healing in HPRCCs have been quite well assessed and understood, the phenomenon being the result of con-

curing (1) delayed hydration of un-hydrated binder because of the quite low initial water–binder ratios and (2) carbonation of calcium hydroxide [32–35].

On the other hand, an assessment of the healing capacity in terms of “correlation” between crack closure, material performance recovery and structural response is far from being provided. This is a much needed concept to be established in view of incorporating self-healing outcomes and benefits into code-format design approaches and it requires the self-healing capacity to be assessed, as this paper aims to do, through more than one tests and in terms of several parameters [13,16,22,36–39], encompassing and cross-referencing the closure of the cracks with the recovery of more than one mechanical and/or durability performance of interest.

## 2. Research significance and experimental campaign

In order to investigate the durability performance of the UHDCs in real service conditions, a multi-test/multi-parameter approach has been adopted aimed at investigating the response of the materials under different conditions, while taking in mind the final engineering application. The project, in fact, foresees also the application of the materials studied (and, more generally, of the approach developed) in full-scale demonstrators (referred as pilots), in which several parameters will be monitored during time. The pilot in which the mixes herein presented will be used is a basin inside a Geothermal Power Plant owned by project partner Enel Green Power and located in Tuscany (Italy) [40].

The prototype is a tank for the collection of water from the cooling towers of the geothermal plant, whose composition, as from Table 1, features high content of both sulphate and chloride ions. The target of such demonstrator is to compare the traditional solution in ordinary concrete and the new one in UHDC, with wall thickness ranging, in the case of UHDC, from 30 to 60 mm.

The experimental campaign has been planned in order to encompass the two-fold objective of providing (1) a first results database for developing the durability-based design framework and (2) an integrated multi-parameter self-healing assessment. To this aim the following three different test setups have been adopted, addressing the recovery brought in cracked samples by self-healing in terms of water permeability, flexural stiffness and crack-sealing:

- water permeability test on 100 mm diameter and 60 mm thick concrete disks;
- 4-point-bending test on Thin Beams - TB (25 × 100 × 500 mm<sup>3</sup>);
- 4-point-bending test on Deep Beams - DB (100 × 100 × 500 mm<sup>3</sup>).

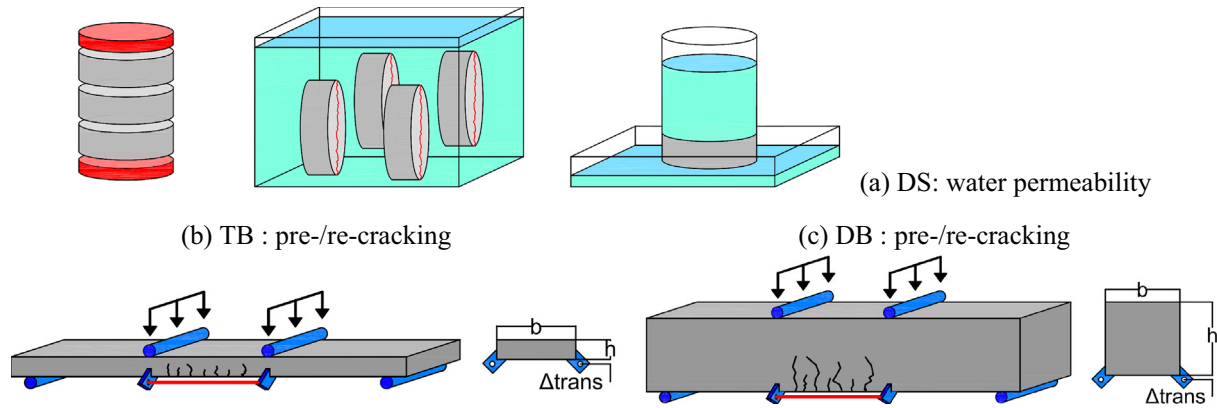
In the first test only water permeability is assessed, while in the other two setups (based of flexural tests) both crack-sealing and stiffness recovery are investigated, as better described in the following.

### 2.1. Water permeability test

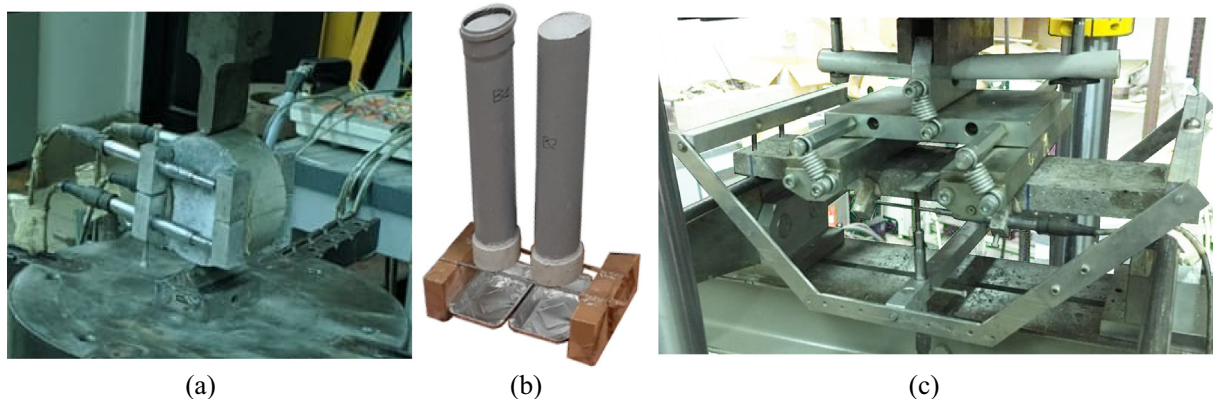
Concrete disks  $\emptyset \times H = 100 \times 60 \text{ mm}^2$  have been obtained by cutting concrete cylinders  $\emptyset \times H = 100 \times 280 \text{ mm}^2$  after removing the two ends (Fig. 1a). Each disk has been then pre-cracked by splitting up to a target residual nominal crack width of  $100 \pm 50 \mu\text{m}$  (Fig. 2a), measured during the test via 3 LVDTs positioned across the fracture plane. Due to the state of stress and to the geometry of the specimen, no multiple cracking has occurred

**Table 1**  
Composition of the geothermal water employed for specimen healing.

Constituent	Al	Ca	Fe	K	Mg	Na	S	Si	SO <sub>4</sub> <sup>2-</sup>	Cl
ppm	0.2	4	0.13	19.8	0.3	1243.2	1523.4	0.3	2678	441



**Fig. 1.** Concrete disks cut from cylinders then stored in geothermal water and finally subjected to water permeability test (a), and 4-point bending test setup for pre-cracking and re-cracking in Thin Beams – TB (b) and Deep Beams – DB (c).



**Fig. 2.** Setup for concrete disks subjected to pre-cracking by splitting (a) and to water permeability test (b), and 4-point bending test for pre-cracking and re-cracking of small beams (c).

and just one single crack has been obtained. Afterwards, the disks have been stored vertically in geothermal water for all the curing time.

Half of the specimens have been cured with continuous immersion in water, while half have been subjected to wet and dry (W/D) cycles, being one week immersed in geothermal water and one week in moist room (90% RH). After 1 and 3 months from pre-cracking, permeability test has been performed by gluing 500 mm-long PVC tubes on the top of the disks (Fig. 2b). The tube has been filled with about 3 L of tap water and the flow through the crack has been monitored by weighing the water dropping down at different time intervals. Finally, permeability factor has been evaluated at the beginning,  $K_0$ , and at the end,  $K_t$ , of curing so to calculate the index of permeability recovery,  $IPRO_0$ :

$$IPRO = 1 - K_t/K_0 \tag{1}$$

**2.2. Four-point bending test**

Thin concrete slabs  $25 \times 500 \times 1000 \text{ mm}^3$  have been cast and then cut into 20 thin beams with the dimensions of  $25 \times 100 \times 500 \text{ mm}^3$ . The procedure of casting slabs and then per-

forming cuts guarantees a better alignment of the fibre with respect to the production of single  $25 \times 100 \times 500 \text{ mm}^3$  specimens [41].

After at least 60 days from casting, specimens have been subjected to 4-point bending test up to the prescribed residual deformation at the bottom side of  $1‰$  (measured after unloading) side of  $1‰$ , namely *pre-cracking*. The use of 4-point bending test rather than 3-point bending test allows multi-cracking, this being representative for materials with strain/deflection-hardening behaviour in their structural service scenario. During the test, the tensile deformation has been measured at the bottom side in the region between the two loading blades by means of two LVDTs positioned between two fixed platelets (Figs. 1b,c and 2c).

After cracking, each crack at the bottom side of the specimens has been identified and recorded via digital microscope. After 1 month from *pre-cracking*, each crack has been recorded again in order to compare the crack just after *pre-cracking* and after 1 month of healing. Afterwards, some specimens have been subjected again to 4-point bending in order to simulate a cyclic crack opening (namely *re-cracking*) by imposing a further crack opening equal to the first one.

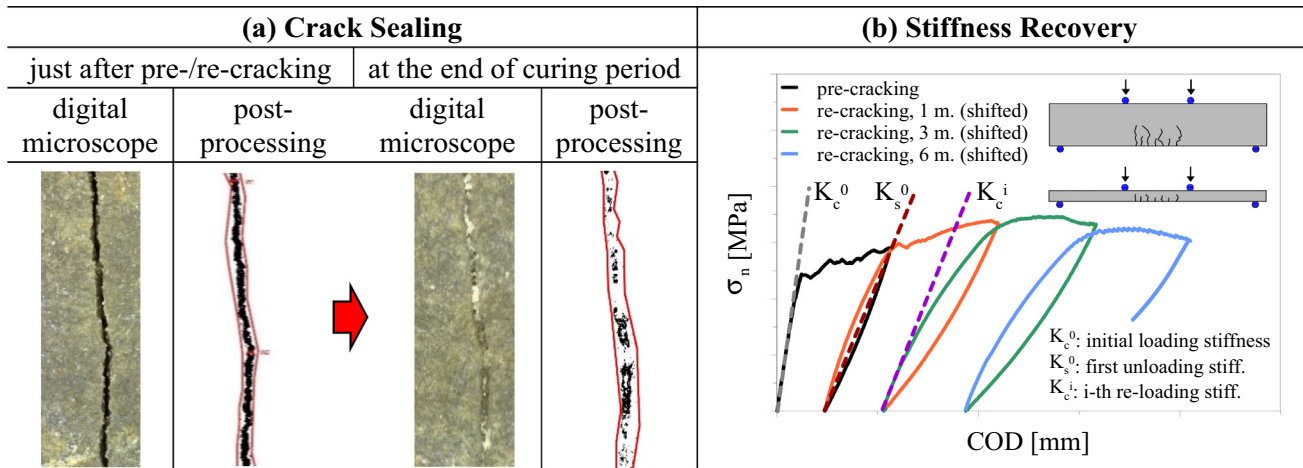


Fig. 3. Sketch of (a) crack area analysis at different healing stages (Index of Crack Sealing – ICS), and (b) loading/unloading slope comparison in pre-/re-cracking curves (Index of Stiffness Recovery – ISR).

All cracks have been recorded again by digital microscope just after *re-cracking* and then checked after further 2 months (at 3 months after first *pre-cracking*). Also in this case *re-cracking* has to be performed in some specimens. Finally, at 6 months after *pre-cracking*, cracks have been recorded again by digital microscope and specimens have been tested up to failure. The optical digital microscope *DinoLite* has been adopted (with a magnification factor of 225) together with the software *DinoLite Capture*.

Crack sealing can be assessed rather quickly via image processing software such as Photoshop®, by extrapolating the crack region as a set of black pixels and so quantifying its area as a function of curing time (Fig. 3a), according to the same methodology explained in detail in [21,42]. Finally, the *Indexes of Crack Sealing* - ICS can be easily computed:

$$ICS_0 = \frac{A_{F,0} - A_{F,i}}{A_{F,0}} \quad (2a)$$

$$ICS_{i-1} = \frac{A_{F,i-1} - A_{F,i}}{A_{F,i-1}} \quad (2b)$$

where  $A_{F0}$  is the crack area just after *pre-cracking*,  $A_{Fi-1}$  is the crack area just after *re-cracking* and  $A_{Fi}$  is the crack area at the end of the healing period. Crack sealing is therefore herein defined as the closing of the external edge of the crack (and not as the rigorous restoration of the same conditions of the uncracked state all along the crack surface).

It is worth noticing that  $ICS_0$  always refers to the crack opening measured at pre-cracking and this index can be evaluated just in the specimens which are not re-cracked, while  $ICS_{i-1}$  addresses self-sealing taking place within each healing period in re-cracked

specimens (for which, on the contrary, the index  $ICS_0$  cannot be estimated).

Tests have been performed in loading-blades displacement control, with a displacement rate of 5  $\mu\text{m/s}$ . At each cracking step (both *pre-cracking* and *re-cracking*), the same residual strain of 1‰ was set as target.

Specimens *re-cracking* at each target time interval makes it possible to evaluate the *Index of Stiffness Recovery* - ISR due to self-healing and calculated according to the following relations:

$$ISR_0 = \frac{K_c^i - K_s^0}{K_c^0 - K_s^0} \quad (3a)$$


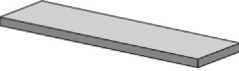
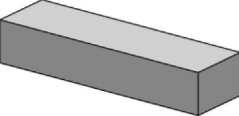
$$ISR_{i-1} = \frac{K_c^i - K_s^{i-1}}{K_c^{i-1} - K_s^{i-1}} \quad (3b)$$

the different parameters being explained in Fig. 3b, where *pre-cracking*  $\sigma$ -COD law (black curve) is reported together with the *re-cracking* curves at 1, 3 and 6 months (respectively, orange, green and light blue curves). The latter three curves are shifted in the COD axis in order to restore the continuity of the diagram [20]. The ISR index can be evaluated only in re-cracked specimens, for which the recovery can be expressed with respect to either the initial *pre-cracking* stage ( $ISR_0$ ) or the previous *re-cracking* stage ( $ISR_{i-1}$ ).

Exact the same procedure has been followed for thicker specimens ( $100 \times 100 \times 500 \text{ mm}^3$ ), with the only difference that specimens were cast on separate moulds.

Testing different specimen geometries aimed at investigating possible scale-effects due to both technological reasons (related to fibres dispersion and alignment) and mechanical aspects (such

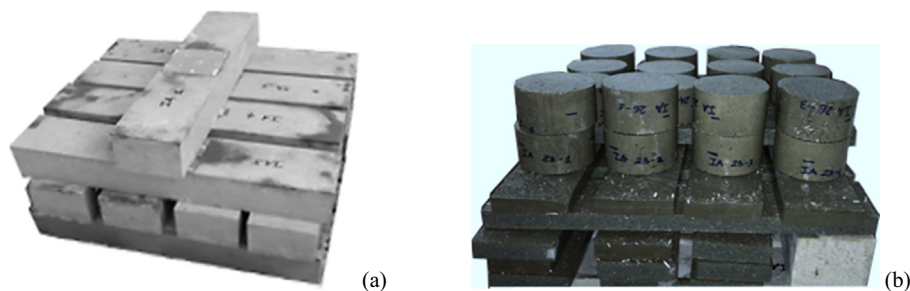
Table 2  
Number of specimens for each geometry and conditioning for self-healing assessment.

specimen geometry	time intervals	cracking mode	tot./rel. number	mechanical conditioning	rel. num.	curing type	Self-Healing Indexes
	0, 1, 3, 6 months	splitting	20 / 20	pre-cracking	10	immersion w/d cycles	IPR <sub>0</sub>
	0, 1, 3, 6 months	4PBT	8 / 8	pre-/re-cracking	8	immersion	ICS <sub>i-1</sub> , ISR <sub>0</sub> , ISR <sub>i-1</sub>
	0, 1, 3, 6 months	4PBT	16 / 6	pre-cracking	3	immersion w/d cycles	ICS <sub>0</sub>
			10	pre-/re-cracking	5	immersion w/d cycles	ICS <sub>i-1</sub> , ISR <sub>0</sub> , ISR <sub>i-1</sub>



**Table 3**  
Investigated UHDC mixes composition. ( $^{\wedge}l_f/d_f = 20/0.2$  mm;  $^*l_f/w_f/t_f = 15/1/0.024$  mm).

		XA-CA	XA-CA-Amf	XA-CA-CEMIII
Cement CEM I 52.5	[kg/m <sup>3</sup> ]	600	600	-
Cement CEM III 52.5	[kg/m <sup>3</sup> ]	-	-	600
Slag	[kg/m <sup>3</sup> ]	500	500	500
Water	[kg/m <sup>3</sup> ]	200	200	200
Steel fibres <sup>^</sup>	[kg/m <sup>3</sup> ]	120	-	120
Amorphous fibre <sup>*</sup>	[kg/m <sup>3</sup> ]	-	111	-
Sand (0–2 mm)	[kg/m <sup>3</sup> ]	982	982	982
Superplasticizer	[kg/m <sup>3</sup> ]	33	33	33
Crystalline admixture	[kg/m <sup>3</sup> ]	4.8	4.8	4.8
Avg cub. compr. strength	[MPa]	137	107	136
Avg flexural peak stress	[MPa]	20.7	20.0	22.4



**Fig. 4.** Deep beams after demoulding (a) and disks and thin beams after cutting (b).

as tensile stress redistribution in the section). In the following,  $25 \times 100 \times 500$  mm<sup>3</sup> samples will be referred as Thin Beams – TB, while  $100 \times 100 \times 500$  mm<sup>3</sup> samples as Deep Beams – DB.

Thin beams have been all cured in continuous immersion in water, while regarding deep beams half of them have been subjected to continuous immersion and half of them to wet and dry (W/D) cycles with one week immersed in geothermal water and one week in moist room (90% RH). Finally, while all thin beams have been re-cracked at each target period (1, 3 and 6 months from pre-cracking), 6 deep beams have been subjected just to pre-cracking and 10 to pre- and re-cracking (see Table 2).

It is worth noting that *re-cracking* allows for assessing the self-healing effectiveness under repeated cracking, this being investigated just in a few studies in the literature [22,26] even though it represents a major concern for many onshore and offshore structures.

### 3. Mixes

As reported in Table 3, the study is based on a reference UHDC mix, containing crystalline admixture Penetron Admix<sup>®</sup> as autogenous healing stimulator (whose benefits in terms of durability and self-healing performances have been investigated elsewhere [8,43]), and identified in the following as XA-CA [6,20].

In order to study the effect of cement and fibre types, other two mixes have been investigated replacing steel fibre with amorphous metal-alloy fibre (XA-CA-AmF) and CEM I with CEM III (XA-CA-CEMIII). In Fig. 4 two pictures of the different specimens prepared for each mix are shown.

### 4. Results and discussion

The mechanical characterization performed in a preliminary experimental campaign (see [41] for the details) by means of 4-point bending tests as well as indirect tension Double Edge Wedge

Splitting tests has demonstrated the strain-hardening behaviour in both direct tension and bending, as anticipated in the introduction. Such behaviour makes it possible that in the flexural tests more than 83% of cracks is characterized by a width lower than 50  $\mu$ m for a tensile strain at the bottom side of 1‰ (see Fig. 5b), this being instrumental for effectively promoting self-healing. The same percentage goes down to 60 and 40% for a tensile strain of 2 and 3‰ (Fig. 5c, d), respectively.

The distribution of crack width is reported in Fig. 5a for disks after pre-cracking, showing as 70% of the cracks are within the target range (50–150  $\mu$ m), while for 20% of cracks the width is larger due to the difficulty in controlling the splitting test after crack localization.

In Fig. 5b, c, d the crack width distribution is reported for deep beams after *pre-* and *re-cracking*, obviously showing as the distribution of crack width moves towards higher values with further *re-cracking*. In some specimens, crack localization (with crack width higher than 100  $\mu$ m) takes place in XA-CA-Amf already at 1-month *re-cracking*, while for the other two mixes this phenomenon starts taking place in a few samples only at 3-month *re-cracking*. In Fig. 6, two pictures show the typical crack pattern for deep and thin beams, which resulted to be very similar.

In Fig. 7 the index of permeability recovery, IPR<sub>0</sub>, is shown as a function of time from *pre-cracking* (1, 3 and 6 months), for mix XA-CA only. It can be observed that water permeability is efficiently recovered already at 1 month from pre-cracking, in both curing conditions (namely, continuous and cyclic immersion), with full recovery at 3 months (this also made the execution of tests at 6 months meaningless, since total recovery can be assumed).

The high healing observed can be ascribed to the narrow width of the cracks that makes it difficult the water flow even before “full” crack sealing takes place. In this regards, it is worth noting that different results could be obtained if water permeability was measured under high pressure [42], where however a complex interaction between water flow and removal of healing products could be observed. The condition of water permeability under

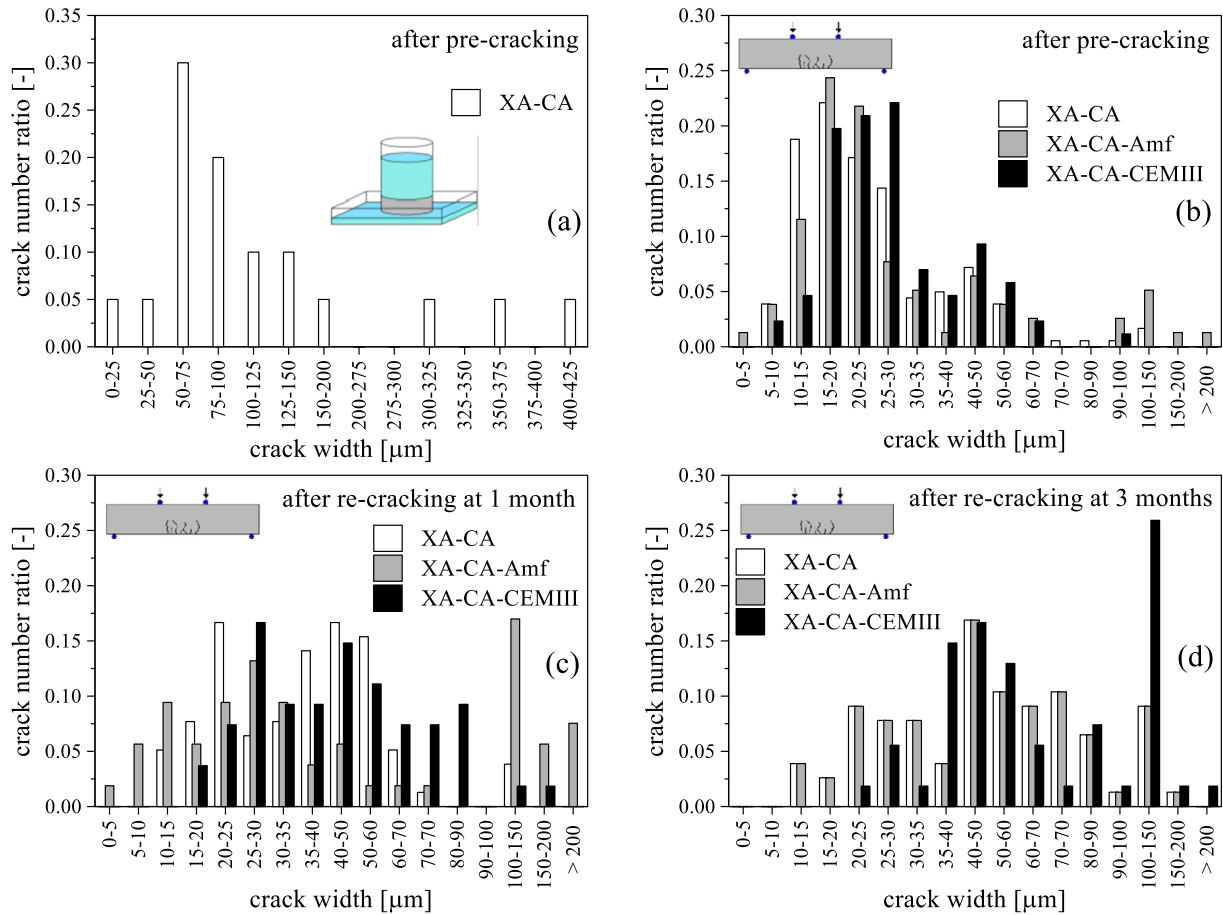


Fig. 5. Crack width distribution in disks after pre-cracking (a) and in deep beams just after pre-cracking (b), after re-cracking at 1 month (c) and at 3 months (d).



Fig. 6. Typical crack patterns after pre-cracking for deep beams (a) and thin beams (b).

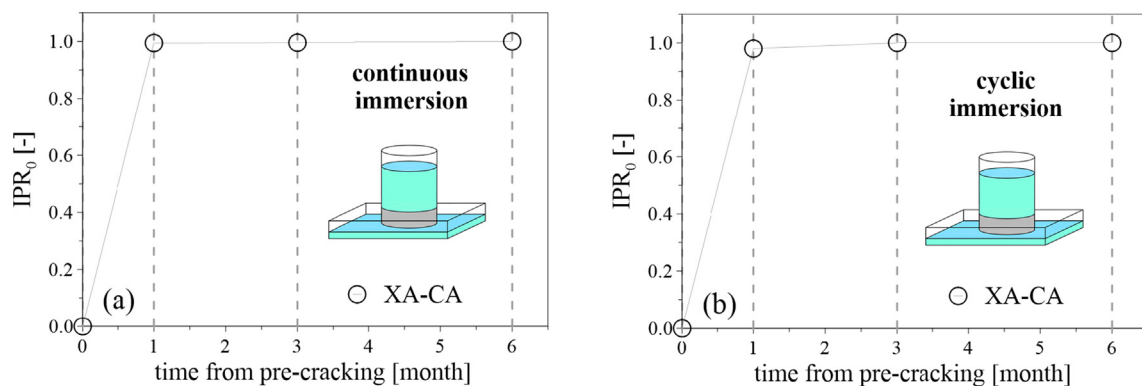
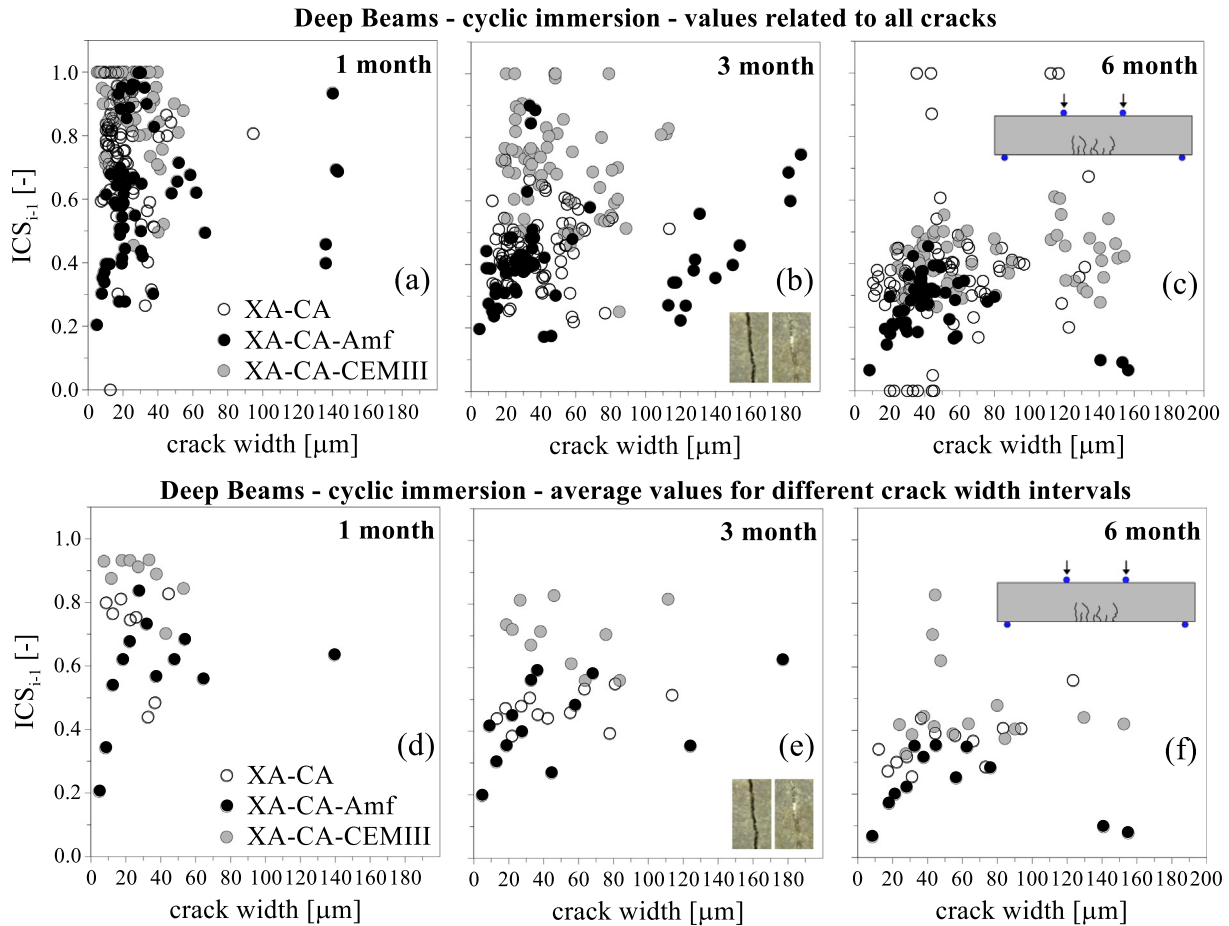


Fig. 7. Index of Permeability Recovery, IPR<sub>0</sub>, for continuous (a) and cyclic (b) immersion in geothermal water for disks.

pressure is, however, not representative of the structural service scenario in the intended pilot application, and this is the reason why it has not been adopted in the present experimental program.

In Fig. 8a, b, c, the index of crack sealing ICS is reported for each crack for the 3 mixes at 1, 3 and 6 months, respectively, in the case of deep beams in cyclic immersion in geothermal water. In Fig. 8d, e, f the same indexes are reported, averaging the values for discrete



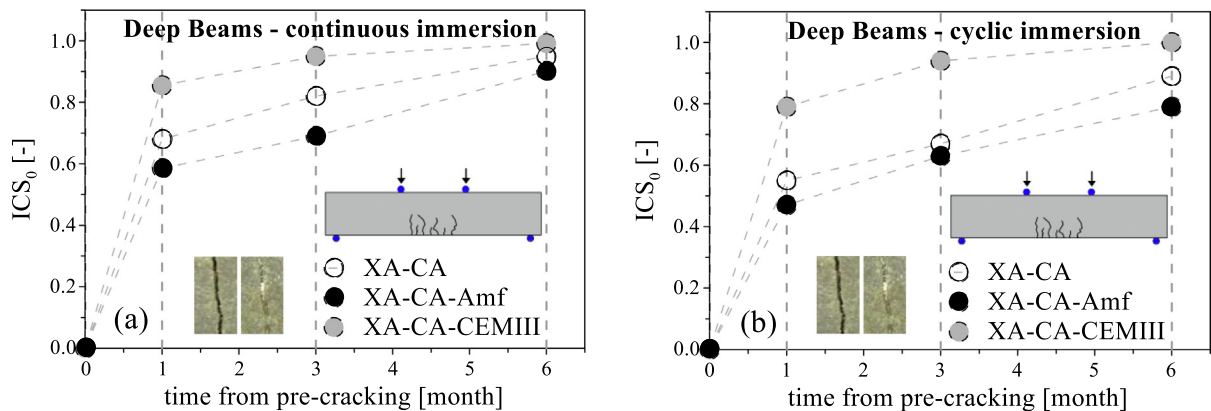
**Fig. 8.** Index of Crack Sealing with respect to previous time step re-cracking,  $ICS_{t-1}$ , for deep beams with W/D cycles, evaluated for each crack after 1 (a), 3 (b) and 6 (c) months from pre-cracking, and correspondent averaged values in discrete crack-width intervals (d, e, f).

crack-width intervals, in order to more easily enlighten any possible trend. As expected, moving from Fig. 8d to f, the crack-width distribution moves towards higher values, while the index ICS shows lower values, due to the partial loss in efficacy in self-healing processes.

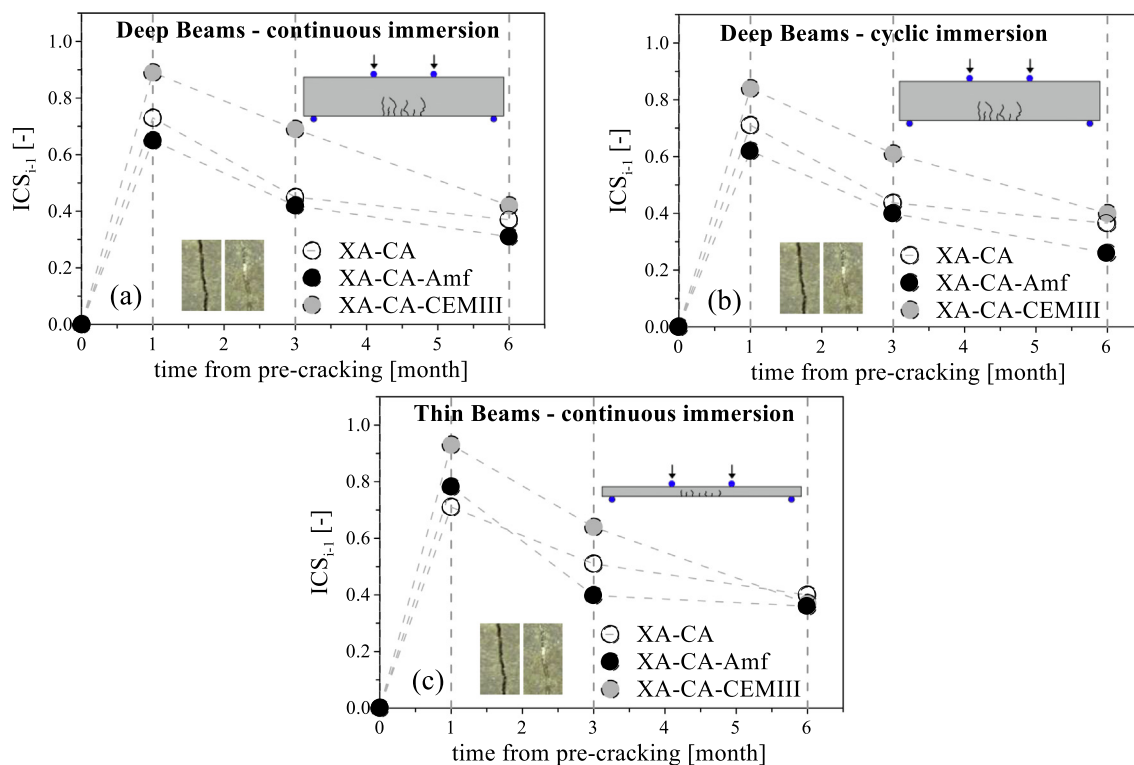
A clear trend of ICS with respect to crack-width cannot be detected, due to the sizable scattering of the results, on the one hand, and to the rather narrow crack-width range investigated, on the other hand. The not clear dependence of ICS index on

crack-width, makes it reasonable to average the ICS values in the whole crack-width range, thus obtaining the plots in Figs. 9 and 10. It is worth noting that for design purposes, reference values can be estimated with higher confidence coefficients than the average, as for example the characteristic value corresponding to the 5th percentile.

In Fig. 9 the average index of crack sealing  $ICS_0$  is reported for the 3 mixes at 1, 3 and 6 months, for deep beams specimens without re-cracking at the different target time intervals, in case of cyc-



**Fig. 9.** Index of Crack Sealing with respect to initial pre-cracking,  $ICS_0$ , in case of (a) continuous and (b) cyclic immersion in geothermal water for DB specimens, without re-cracking.



**Fig. 10.** Index of Crack Sealing with respect to previous time step re-cracking,  $ICS_{i-1}$ , in case of TB and DB specimens under cyclic or continuous immersion in geothermal water.

lic and continuous immersion in geothermal water. In this case the index is evaluated with respect to initial pre-cracking (time 0), this being the reason why it increases with time.

As a matter of fact, it appears that crack sealing is very effective in the first month of curing, with a percentage of crack closing in the range 57–84% for continuous immersion and 47–80% for cyclic immersion. As expected, healing is more effective in the case of continuous immersion thanks to the larger availability of water, which is necessary for the precipitation of healing products. Between 1 and 3 months of curing, the further crack closing in case of re-cracking is in the range 11–14% for continuous immersion and 12–16% for cyclic immersion.

The slowing down of healing phenomenon is due to (1) the progressive precipitation in the healing process, which makes more difficult the ingress of new water/moisture for further healing, and (2) the lower availability of un-hydrated cement grains. In the final stage, between 3 and 6 months of curing the further crack closing is in the range 4–20% for continuous immersion and 6–22% for cyclic immersion.

In Fig. 10 the index of crack sealing  $ICS_{i-1}$  is shown for the 3 investigated mixes at 1, 3 and 6 months regarding specimens with re-cracking, for deep beam specimens in case of cyclic and continuous immersion in geothermal water and for thin beam specimens in case of continuous immersion in geothermal water. The index is evaluated with respect to previous re-cracking loading curve (0 to 1 month, 1 to 3 months and 3 to 6 months), this explaining why it tends to decrease with time.

Similar comments as for  $ICS_0$  also hold in this case of index  $ICS_{i-1}$ , where crack closing ratio is in the range 65–93% for continuous immersion and 62–84% for cyclic immersion in the first month, 40–69% and 40–61% between months 1 and 3, and 31–42% and 26–40% between months 3 and 6.

Also in this case it is confirmed as continuous immersion in geothermal water has a beneficial effect with respect to cyclic

immersion, thanks to the higher availability of water for the healing process. In both Figs. 9 and 10 it is shown as the best performance is provided by XA-CA-CEMIII and the worst by XA-CA-Amf, as better discussed in the following.

In Fig. 11a, the index of stiffness recovery with respect to initial pre-cracking,  $ISR_0$ , is shown as a function of the residual COD, in the case of deep beams with curing in continuous immersion in geothermal water. Each point in the plot refers to a single specimen. It can be noted a non-negligible scattering with respect to the target residual COD (150, 300 and 450  $\mu\text{m}$  at 1, 3 and 6 months, respectively), which allows to highlight a clear relationship between  $ISR_0$  and residual COD, the former decreasing for increasing values of the latter. Averaging the  $ISR$  values for each target curing time (1, 3 and 6 months), it is possible to work out the synthetic plot reported in Fig. 11b. In Fig. 11b, c, d, the average index of stiffness recovery with respect to initial pre-cracking,  $ISR_0$ , is shown in case of continuous or cyclic immersion in geothermal water for deep and thin beams with re-cracking. In Fig. 12a, b, c it is reported the corresponding index of stiffness recovery with respect to previous re-cracking immersion.

In this case, the healing process appears to be more complex, as far as the stiffness recovery is concerned, since Fig. 11 shows an increase of  $ISR_0$  in the first month and a decrease between month 1 and 3. This can be ascribed to the fact that the damage introduced by re-cracking at 1 month is not fully recovered in the 2 following months of curing. In the range 3–6 months, on the other hand, the index keeps again growing thanks to the higher curing time. The final stiffness recovery is, however, rather important, being even higher than 80% in case of continuous immersion. This significant healing is favoured by the beneficial effects brought in by the crystalline admixture. The results are aligned with other studies focused on engineered cementitious materials [22,26], despite in the present case specimens are subjected to aggressive conditions in the healing period.



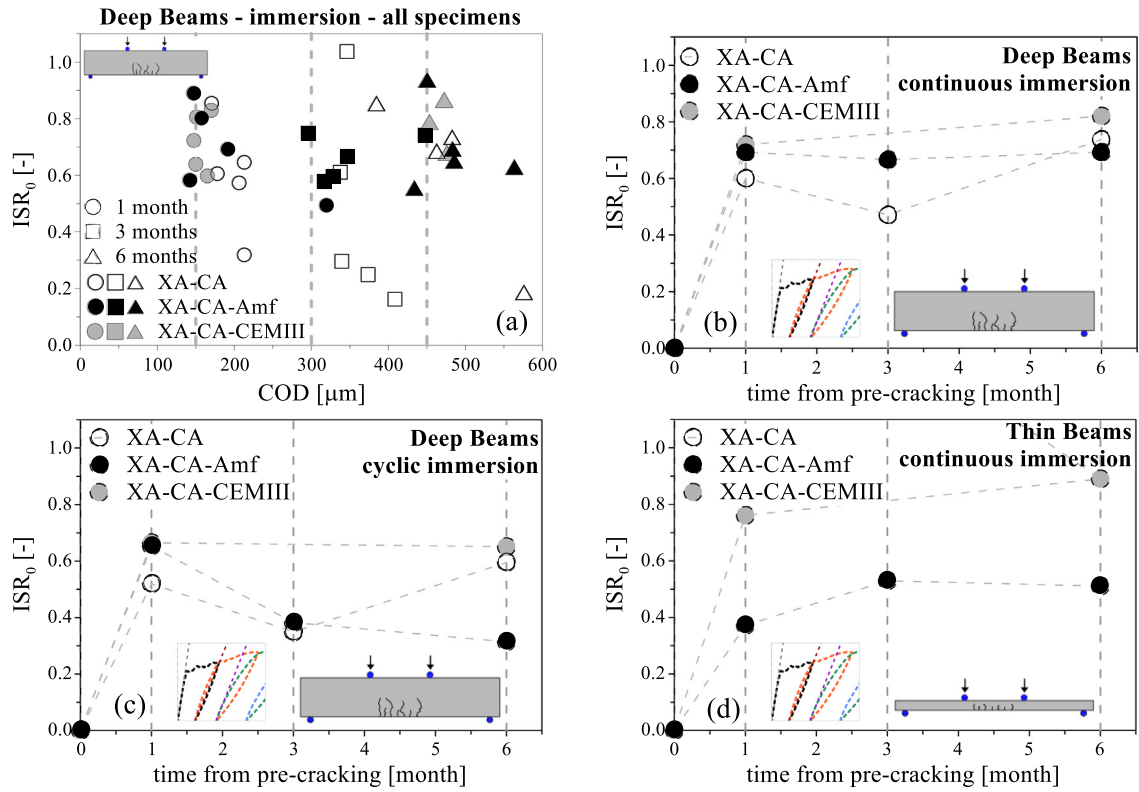


Fig. 11. Index of Stiffness Recovery with respect to initial pre-cracking,  $ISR_0$ , for each specimens in case of DB in continuous immersion in water as a function of residual COD (a), and averaged values for the target curing time intervals for DB and TB specimens in case of continuous or cyclic immersion in geothermal water (b, c, d), with re-cracking.

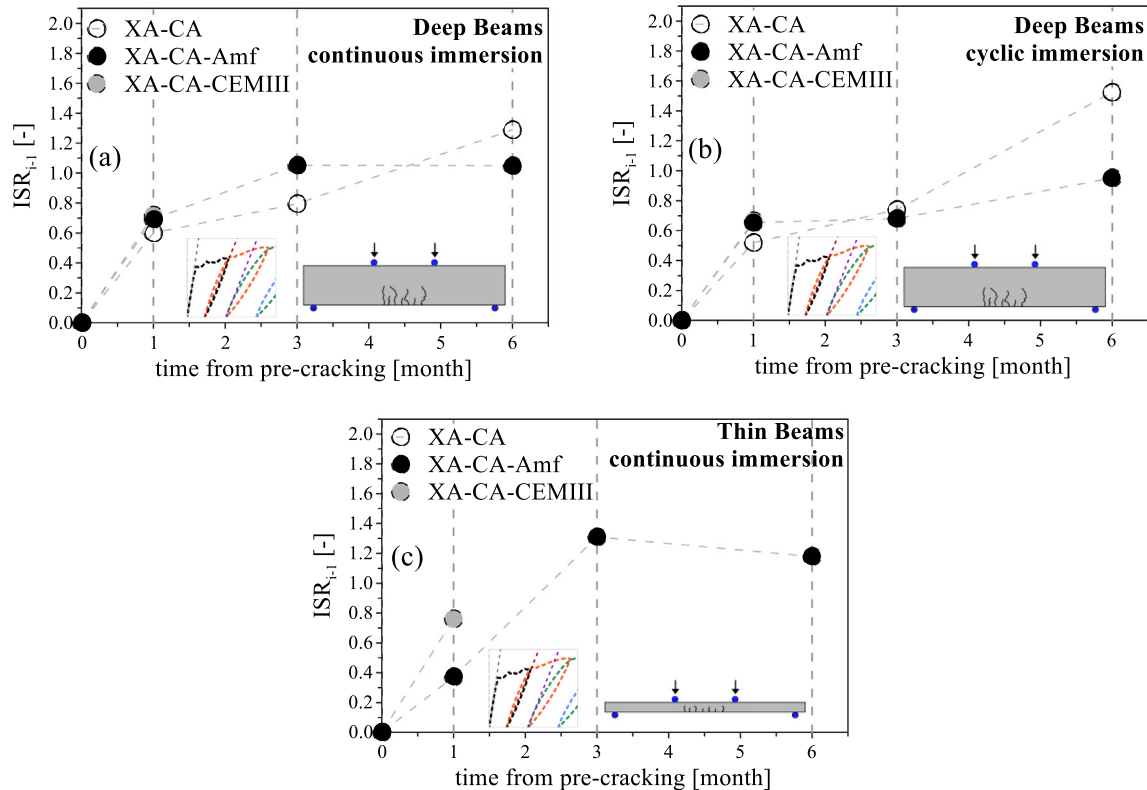


Fig. 12. Index of Stiffness Recovery with respect to previous time step re-cracking,  $ISR_{i-1}$ , for DB and TB specimens in case of continuous or cyclic immersion in geothermal water, with re-cracking.

Slightly different results are provided by the index  $ISR_{i-1}$ , which shows a continuous increase of the healing level. The difference with respect to the index  $ISR_0$ , however, depends on the fact that index  $ISR_{i-1}$  takes into account also the degradation of the final unloading slope  $K_s^{-1}$ . Hence, in the index  $ISR_{i-1}$ , the apparent increase is caused by the fact that the unloading slope decreases more than the loading branch, this showing just an apparent increase of the healing level.

Summarizing, comparing the results shown in Figs. 7–12, it is clear as the most performing mix in terms of crack-sealing is XA-CA-CEMIII, while the worst performance is provided by XA-CA-Amf. The better performance of XA-CA-CEMIII is ascribed to the large amount of slag, which provides higher quantity of unhydrated (but reactive) products even at long curing time, thus fostering self-healing.

On the other hand, the worse outcome from XA-CA-Amf is linked to the larger initial average crack opening probably caused by the less effective crack-bridging effect of amorphous fibres (see also [41]), as shown in Fig. 5 especially after pre-cracking and 1-month re-cracking. The mix UHDC XA-CA is in between the other two mixes.

It can be remarked, however, that (a) all the mixes prove a very good performance with reference to crack self-sealing (with the recovery indexes higher than 80% without re-cracking and around 40% with re-cracking) and (b) the difference among the three mixes becomes less and less sizable for longer curing durations.

Finally, in Fig. 13 the correlation between indexes  $IPR_0$ ,  $ICS_0$  and  $ISR_0$ , namely permeability recovery, crack sealing and stiffness recovery, is reported with reference to deep beams in case of cyclic or continuous immersion.

It can be observed as permeability recovery provides the highest values, since full recovery can be attained even though the crack is not completely sealed thanks to the fact that water flow is already made negligible for very small crack width. On the other hand, stiffness recovery is lower than the correspondent crack-sealing index. This result is reasonable, since crack-sealing index is mostly sensitive to self-healing process occurring at the crack external edges (where healing is fostered by the higher amount of accessible water), while stiffness-recovery index sees also the healing process involving the inner region of cracks and the fibre-matrix bond.

Once again it is worth noting the detrimental role of cyclic cracking (herein referred as re-cracking), whose effect has been considered in the present study and which represents a critical issue in the design phase of real structures. This proves as it must be properly considered in the development of a Durability-Assessment based Design – DAD.

### 5. Conclusions

In the present paper, the experimental assessment of self-healing via different test setups is described regarding three Ultra-High Performance Fibre Reinforced Cement Composites developed within the framework of the European Project ReSHEALiencie. In particular, a multi-test/multi-parameter approach has been adopted aimed, on the one hand, at better investigating the effect of self-healing on different concrete properties and, on the other hand, at providing a preliminary data base instrumental for properly and systematically taking into account self-healing in structural design.

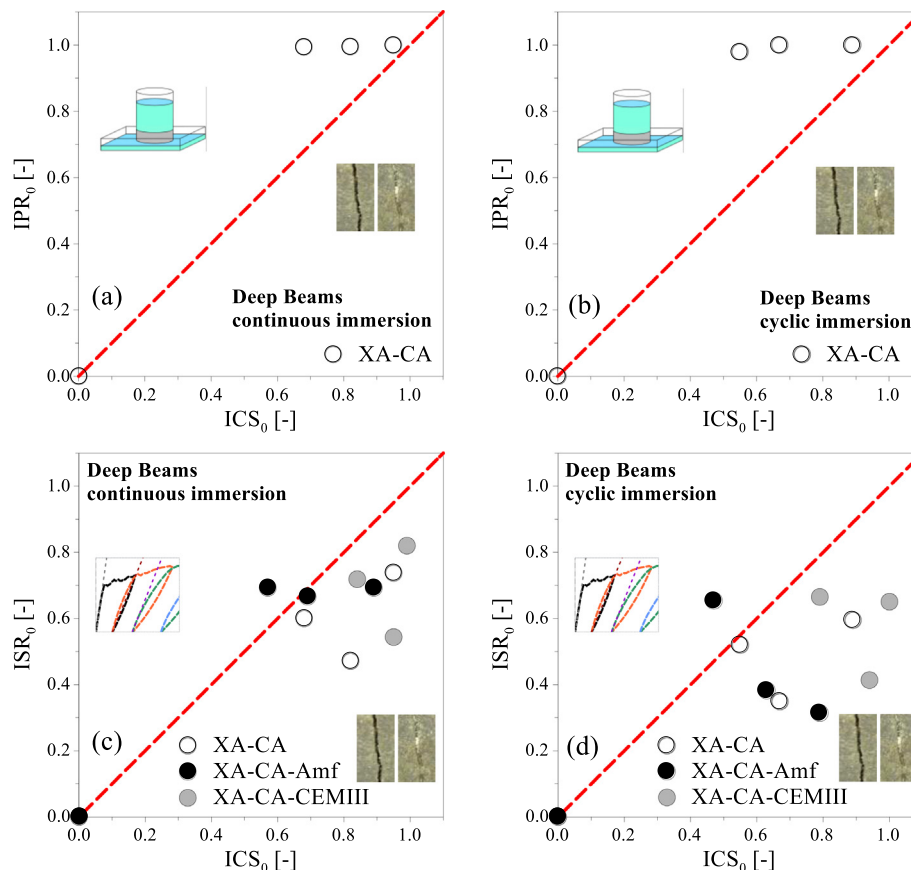


Fig. 13. Correlation between indexes  $IPR_0$  and  $ICS_0$ , and between  $ICS_0$  and  $ISR_0$ , for DB specimens in case of continuous or cyclic immersion in geothermal water.

In details, three main material parameters have been analysed, namely *permeability recovery*, *crack-sealing capability* and *stiffness recovery*. The study has involved both pre-cracked and re-cracked specimens, subjected to two different aggressive curing conditions, namely continuous immersion or wet/dry cycles in geothermal water. For each of the three material parameters, a synthetic self-healing index has been formulated with the aim of monitoring its variation as a function of curing time.

Based on the evaluations presented, the following conclusions can be drawn:

- the adoption of strain-hardening cement composites promotes self-healing phenomenon, thanks to smeared cracking in the tensile region, with low values of crack opening (in the range 10–50  $\mu\text{m}$  for a tensile strain of 1‰, in the present study);
- the multi-test/multi-parameter approach adopted for the self-healing assessment of the mixes appeared to be robust and able to provide useful data instrumental for durability assessment in structures, regarding water permeability, crack-sealing capability and mechanical recovery;
- self-healing is very effective already after 1 month of curing (with values generally higher than 70% for XA-CA-CEMIII for all the parameters investigated), while afterwards its increase is smoothed down due to the fact that water is made less accessible to the surface of concrete, where new healing products can be formed;
- all the three mixes investigated showed sizable self-healing, with almost full crack-sealing after 6 months in absence of *re-cracking* and at least 40% recovery in case of *re-cracking*;
- considering all the three parameters investigated, the most performing mix in terms of self-healing is UHDC XA-CA-CEMIII thanks to the large amount of slag (which provides higher quantity of un-hydrated, but reactive, products), while the worst is UHDC XA-CA-Amf due to the initial larger average crack opening. The mix UHDC XA-CA is in between the other two mixes;
- the material parameter that shows the highest values of healing is permeability, thanks to the fact that water flow is already made negligible for very small crack width. On the other hand, the property which proved to be most hardly fully-recovered is stiffness, since it is sensitive to the healing effectiveness along the whole crack-surface. Finally, crack-sealing index shows to be in between, since it is affected by the healing process occurring just at the crack external edges (where healing is fostered by the higher amount of accessible water);
- the detrimental role of cyclic re-cracking has been highlighted, showing an overall decrease for all the parameters investigated.

The approach herein discussed and the results above reported represent a promising starting point for the development of a Durability-Assessment-based Design – DAD, in which self-healing can be explicitly taken into account, thus making possible the exploitation of the huge benefits brought in by the use of advanced cementitious materials. In this regard, however, the proper evaluation of the sensitivity and of the repeatability of the experimental tests adopted for self-healing assessment plays a major role. To this end, the Authors are active in the EU COST Action CA 15,202 “Self-healing as preventive repair of concrete structures – SARCOS”, in which self-healing experimental assessment is a major topic.

#### CRedit authorship contribution statement

**Francesco Lo Monte:** Conceptualization, Data curation, Writing – original draft. **Liberato Ferrara:** Conceptualization, Supervision.

#### Declaration of Competing Interest

The authors declare that they have no known competing financial interests or personal relationships that could have appeared to influence the work reported in this paper.

#### Acknowledgements

The activity described in this paper has been performed in the framework of the project “Rethinking coastal defence and Green-energy Service infrastructures through enHancEd-durAbiLity high-performance cement-based materials – ReSHEAlience”, funded by the European Union Horizon 2020 research and innovation programme under GA No 760824.

The logistic and technical support of LPM (Laboratory of Material and Structural Testing) at Politecnico di Milano is acknowledged, and in particular Antonio Cocco and Paolo Broglia who actively helped in casting and preparing all the specimens. The authors wish to thank Angelo Alferi, Nicola Borgioni, Andrea Cervini, Luca Famiani, Lorenzo Papa and Stefano Passoni, who passionately contributed to this study in partial fulfilment of their MS degree requirements at Politecnico di Milano.

The kind collaboration of ReSHEAlience partners Penetron Italia (Mr. Enrico Maria Gastaldo Brac) in supplying the crystalline self-healing promoter and Enel Green Power in allowing visits to geothermal plants in Tuscany for geothermal water supply is also acknowledged.

The authors also thank Buzzi Unicem for supplying of cements, Azichem Ltd for supplying of steel fibres and BASF Italia for supplying the superplasticizer employed for casting the different investigated UHDC mixes.

#### References

- [1] S. Matthews, CONREPNET: performance-based approach to the remediation of reinforced concrete structures: achieving durable repaired concrete structures, *J. Build. Appraisal* 3 (1) (2007) 6–20.
- [2] V.H. Perry, What really is ultra-high performance concrete? - Towards a global definition, in: C. Shi, B. Chen (Eds.), Proceedings of the 2nd International Conference of UHPC Materials and Structures, UHPC 2018, Fuzhou, China, November 7–10, 2018, RILEM Pubs, pp. 89–105.
- [3] E. Cuenca, A. Mezzena, L. Ferrara, Synergy between crystalline admixtures and nano-constituents in enhancing autogenous healing capacity of cementitious composites under cracking and healing cycles in aggressive waters, accepted for publication in *Construction and Building Materials*, vol. 266 part B, January 2021, paper 121447, pp. 1–17, <https://doi.org/10.1016/j.conbuildmat.2020.121447>
- [4] N. De Belie, E. Gruyaert, A. Al-Tabbaa, P. Antonaci, C. Baera, D. Bajare, A. Darquennes, R. Davies, L. Ferrara, T. Jefferson, C. Litina, B. Miljevic, A. Otlewska, J. Ranogajec, M. Roig-Flores, K. Pain, P. Lukowski, P. Serna, J.M. Tulliani, S. Vucetic, J. Wang, H.M. Jonkers, A review of self-healing concrete for damage management of structures, *Adv. Mater. Interfaces* 5 (17) (2018) 1–28, <https://doi.org/10.1002/admi.201800074>.
- [5] L. Ferrara, T. Van Mullem, M.C. Alonso, P. Antonaci, R.P. Borg, E. Cuenca, A. Jefferson, P.L. Ng, A. Peled, M. Roig, M. Sanchez, C. Schroefl, P. Serna, D. Snoeck, J.M. Tulliani, N. De Belie, Experimental characterization of the self-healing capacity of cement based materials and its effects on the material performance: a state of the art report by COST Action SARCOS WG2, *Constr. Build. Mater.* 167 (10) (April 2018) 115–142.
- [6] L. Ferrara, V. Krelani, M. Carsana, A fracture testing based approach to assess crack healing of concrete with and without crystalline admixtures”, *Constr. Build. Mater.* 68 (2014) 515–531.
- [7] R.P. Borg, E. Cuenca, E.M. Gastaldo Brac, L. Ferrara, Crack sealing capacity in chloride rich environments of mortars containing different cement substitutes and crystalline admixtures, *J. Sustainable Cem. Based Mater.* 7 (3) (2018) 141–159.
- [8] E. Cuenca, S. Rigamonti, E. Gastaldo Brac, L. Ferrara, Improving resistance of cracked concrete to chloride diffusion through “healing stimulating” crystalline admixtures, *ASCE J. Mater. Civil Eng.* 33 (3) (March 2021) 1–14, [https://doi.org/10.1061/\(ASCE\)MT.1943-5533.0003604](https://doi.org/10.1061/(ASCE)MT.1943-5533.0003604), paper 04020491.
- [9] V.C. Li, H.C. Wu, Conditions for pseudo strain-hardening in fiber reinforced brittle matrix composites, *Appl. Mech. Rev.* 45 (8) (1992) 390–398.
- [10] V.C. Li, H. Stang, H. Krenchel, Micromechanics of crack bridging in fibre-reinforced concrete, *Mats. Struct.* 26 (8) (1993) 486–494.

- [11] V.C. Li, On engineered cementitious composites. A review of the material and its applications, *J. Adv. Concr. Tech.* 1 (3) (2003) 215–230.
- [12] A.E. Naaman, H.W. Reinhardt, Proposed classification of HPFRC composites based on their tensile response, *Mats. Structs.* 39 (5) (2006) 547–555.
- [13] V. Li, Y. Lim, Y. Chan, Feasibility of a passive smart self-healing cementitious composite, *Comp. B: Eng.* 29 (1998) 819–827.
- [14] Y. Yang, M. Lepech, E. Yang, V. Li, Autogenous healing of engineered cementitious composites under wet-dry cycles, *Cem. Concr. Res.* 39 (2009) 382–390.
- [15] Y. Yang, E.-H. Yang, V.C. Li, Autogenous healing of engineered cementitious composites at early age, *Cem. Concr. Res.* 41 (2011) 176–183.
- [16] M. Li, V. Li, Cracking and healing of engineered cementitious composites under chloride environment, *ACI Mats. J.* 108 (3) (2011) 333–340.
- [17] E. Özbay, M. Şahmaran, M. Lachemi, H. Yücel, Self-healing of microcracks in high volume fly ash incorporated engineered cementitious composites, *ACI Mat. J.* 110 (2013) 33–44.
- [18] Z. Zhang, S. Qian, S. Ma, Investigating mechanical properties and self-healing behavior of micro-cracked ECC with different volume of fly ash, *Constr. Build. Mats* 52 (2014) 17–23.
- [19] L. Ferrara, S.R. Ferreira, V. Krelani, M. Della Torre, F. Silva, R. Toledo, Natural fibers as promoters of autogenous healing in HPFRCCs: results from on-going Brazil-Italy cooperation, in: M.A. Chiorino et al. (Eds.), *ACI SP-305. Proc. DSCS, Bologna, Italy, Oct. 1-3 2015*, 11.1-11.10.
- [20] L. Ferrara, V. Krelani, F. Moretti, Autogenous healing on the recovery of mechanical performance of HPFRCCs: part 2 – correlation between healing of mechanical performance and crack sealing, *Cem. Concr. Comp.* 73 (2016) 299–315.
- [21] L. Ferrara, V. Krelani, F. Moretti, M. Roig Flores, P. Serna Ros, Effects of autogenous healing on the recovery of mechanical performance of HPFRCCs: part 1, *Cem. Concr. Comp.* 83 (2017) 76–100.
- [22] M. Şahmaran, G. Yildirim, R. Noori, E. Ozbay, M. Lachemi, Repeatability and pervasiveness of self-healing in engineered cementitious composites, *ACI Mats. J.* 112 (4) (2015) 513–522.
- [23] G. Yildirim, Ö. Kasap Keskin, S. Bahadır Keskin, S. Şahmaran, M. Lachemi, A review of intrinsic self-healing capability of engineered cementitious composites: recovery of transport and mechanical properties, *Constr. Bldg. Mats.* 101 (2015) 10–21.
- [24] G. Yildirim, A. Alyousif, M. Şahmaran, M. Lachemi, Assessing the self-healing capability of cementitious composites under increasing sustained loading, *Adv. Cem. Res.* 27 (10) (2015) 581–592.
- [25] G. Yildirim, M. Şahmaran, M. Balcikanlib, E. Ozbay, M. Lachemi, Influence of cracking and healing on the gas permeability of cementitious composites, *Constr. Bldg. Mats.* 85 (2015) 217–226.
- [26] D. Snoeck, N. De Belie, Repeated autogenous healing in strain-hardening cementitious composites by using superabsorbent polymers, *ASCE J. Mats. Civ. Engrg.* 28 (1) (2016) 1–11.
- [27] D. Snoeck, K. Van Tittelboom, S. Steupaert, P. Dubruel, N. De Belie, Self-healing cementitious materials by the combination of microfibers and superabsorbent polymers, *J. Intell. Mater. Syst. Struct.* 25 (1) (2014) 13–24.
- [28] D. Snoeck, N. De Belie, From straw in bricks to modern use of microfibers in cementitious composites for improved autogenous healing. A review, *Constr. Build. Mater.* 95 (2015) 774–787.
- [29] D. Snoeck, P. Smetryns, N. De Belie, Improved multiple cracking and autogenous healing in cementitious materials by means of chemically-treated natural fibres, *Biosyst. Eng.* 139 (2015) 87–99.
- [30] P. Escoffres, C. Desmettre, J.-P. Charron, Effect of a crystalline admixture on the self-healing capability of high-performance fiber reinforced concretes in service conditions, *Constr. Build. Mater.* 173 (2018) 763–774.
- [31] D. Homma, H. Mihashi, T. Nishiwaki, Self-healing capability of fibre reinforced cementitious composites, *J. Adv. Concr. Technol.* 7 (2) (2009) 217–228.
- [32] D. Kim, S. Kang, T. Ahn, Mechanical characterization of high-performance steel-fiber reinforced cement composites with self-healing effect, *Materials* 7 (1) (2014) 508–526.
- [33] M. Şahmaran, G. Yildirim, T.K. Erdem, Self-healing capability of cementitious composites incorporating different supplementary cementitious materials, *Cem. Concr. Compos.* 35 (2013) 89–101.
- [34] L. Ferrara, S.R. Ferreira, V. Krelani, P. Lima, F.de A. Silva, R.D. Toledo Filho, Cementitious composites reinforced with natural fibers, in: J.A.O. Barros (Ed.), *Recent advances on green concrete for structural purposes. The contribution of the EU-FP7 project EnCoRe*, Springer, 2017, p. 427+x.
- [35] E. Özbay, M. Şahmaran, H. Yücel, T. Erdem, M. Lachemi, V. Li, Effect of sustained flexural loading on self-healing of engineered cementitious composites, *J. Adv. Concr. Technol.* 11 (2013) 167–179.
- [36] M. Şahmaran, S.B. Keskin, G. Ozerkan, et al., Self-healing of mechanically-loaded self-consolidating concretes with high volumes of fly ash, *Cem. Concr. Compos.* 30 (10) (2008) 872–879.
- [37] M. Şahmaran, V. Li, Durability of mechanically loaded engineered cementitious composites under highly alkaline environments, *Cem. Concr. Compos.* 30 (2008) 72–81.
- [38] T. Nishiwaki, S. Kwon, D. Homma, M. Yamada, H. Mihashi, Self-healing capability of fiber-reinforced cementitious composites for recovery of water-tightness and mechanical properties, *Materials* 7 (2014) 2141–2154.
- [39] E. Cuenca, L. Ferrara, Self-healing capability of fiber reinforced concretes. State of the art and perspectives, *J. Korean Soc. Civil Eng.* 21 (7) (2017) 2777–2789.
- [40] S. Al-Obaidi, P. Bamonte, M. Luchini, I. Mazzantini, L. Ferrara, Durability-based design of structures made with UHP/UHDC in extremely aggressive scenarios: application to a geothermal water basin case study, *MDPI Infrastruct.* 5 (11) (November 2020) 1–44, <https://doi.org/10.3390/infrastructures5110102>.
- [41] F. Lo Monte, L. Ferrara, Tensile behaviour identification in ultra-high performance fibre reinforced cementitious composites: indirect tension tests and back analysis of flexural test results, *Mater. Struct.* 53 (145) (2020) 1–12.
- [42] E. Cuenca, A. Tejedor, L. Ferrara, A methodology to assess crack sealing effectiveness of crystalline admixtures under repeated cracking-healing cycles, *Constr. Build. Mater.* 179 (2018) 619–632.
- [43] M. Roig-Flores, S. Moscato, P. Serna, L. Ferrara, Self-healing capability of concrete with crystalline admixtures in different environments, *Constr. Build. Mater.* 86 (2015) 1–11.